MEMS-Based Spectral Decomposition of Acoustic Signals

M. Kranz[1], M.G. Allen[2], and T. Hudson[3]
[1]EngeniusMicro, LLC., Huntsville, AL, USA
[2]Georgia Institute of Technology, Atlanta, GA, USA
[3]U.S. Army AMRDEC, Huntsville, AL, USA

ABSTRACT

Many embedded structural monitoring applications require extremely low-power sensors and signal processing capabilities. In particular, the continuous monitoring of vibrations, impacts, and acoustic noise within a structure typically requires significant power for not only the transducers themselves, but also the signal conditioning, analog to digital conversion, and digital signal processing necessary to extract useful information from the captured waveforms [1,2,3,4]. This paper presents a sensor methodology that performs spectral decomposition of acoustic and vibration waveforms using arrays of micromechanical resonant structures, mechanical filters, and embedded active films, with signal processing being performed in the mechanical domain. The use of embedded active films in these devices results in sensors that can be, in some instances, self-powered by the vibrations being detected. A MEMS-based acoustic emission spectral sensor employing an embedded electret film has been fabricated and tested in an impact environment. Sensor fabrication was performed using *in situ* polarization of the active film after completing the entire fabrication flow. This sensor consisted of an array of tuned micromechanical resonant elements with natural frequencies varying across the spectrum of interest. The sensor was incorporated into a ball drop apparatus in which controlled acoustic pulses could be delivered to the structure under test. Spectral output from the sensor was collected and could be used to distinguish between impacts involving different material sets and impact energies without the use of digital signal processing and its associated power consumption.

Keywords: Ultrasonic Sensor, Mechanical Spectrum Analysis, Ultrasonic Array, MEMS Acoustic Emission

1. INTRODUCTION

This paper presents spectrally sensitive acoustic emission transducers for the detection of various phenomena of interest in monitoring structural system health. Many of the intended applications are volume and power constrained, making it difficult to implement a broadband sensor, data acquisition system, and spectrum analyzer in a small package. Therefore, there is interest in frequency-selective MEMS devices that can perform the spectral analysis within their structure, completely in parallel, while providing an output that is a spectral signal rather than a time domain waveform. This particular effort is investigating electroactive polymer-based structures, in the form of polymer electrets, as acoustic emission transducers in these spectral sensors.

Acoustic emission transducers have commonly been made out of dielectrics configured with parallel-plate capacitor electrodes or piezoelectric elements metalized on both sides. Both of these arrangements provide a current-mode output that is a direct measurement of the acoustic emission signal. In general, the output is proportional to the derivative of the stress propagating through the sensor element. These sensor elements are typically thin or thick films, leading to broadband response. To perform mechanical processing of acoustic signals, a much lower frequency resonance must be achieved. One approach is to use polymer electret materials in a micromechanical resonant structure for the acoustic emission sensors, and to use micromachining to realize resonant behavior at lower frequencies.

An electret, the electrostatic analog of a magnet, is a material with a quasi-permanent electrostatic polarization. Electrets can be fabricated from organic or inorganic materials, with polymers including Mylar and Teflon being commonly employed. Films can be used directly as sensors [5, 6], in a fashion similar to piezoelectric films, or as a bias for sensors or power harvesters [7, 8]. Through the large remnant voltage seen across its surface, an electret can provide a permanent voltage to a moveable sensor electrode. This approach is used in the electret microphone, wherein the electret biases a movable diaphragm. Acoustic waves incident on the diaphragm move it with respect to the electret film, thereby creating a change in the electric field and a measurable output. Similarly, in energy harvesters, the electret film is often used to bias a mass that, when moves, leads to a current flow through an external circuit.

Sensors and Smart Structures Technologies for Civil, Mechanical, and Aerospace Systems 2012,
edited by Masayoshi Tomizuka, Chung-Bang Yun, Jerome P. Lynch, Proc. of SPIE Vol. 8345,
83452U · © 2012 SPIE · CCC code: 0277-786X/12/$18 · doi: 10.1117/12.915408

2. SENSOR DESIGN

For array-based acoustic emission signal processing, an array of electret films and electret-biased MEMS structures were designed as shown in Figure 1. The sensor device under consideration consists of simple metal bridges suspended above a charging grid and polymer film. Once polarized, the electret film creates a voltage bias that capacitively couples with the suspended metal bridge. As the bridge experiences motion, a displacement current is generated in an external circuit. Since polymer-based electrets cannot undergo high temperature processing after being charged, an integrated charging grid is fabricated within the structure to perform *in situ* microcorona charging of the electret polymer after completing device fabrication and packaging.

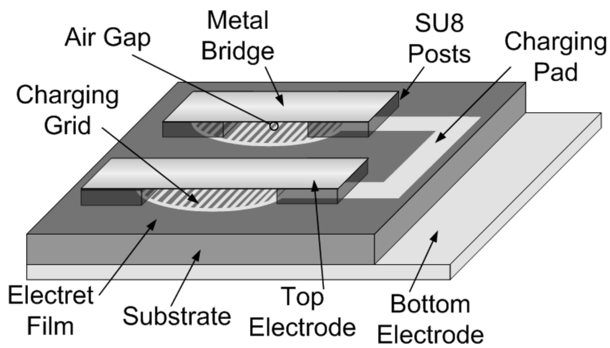

Figure 1: *In Situ* Polarized Electret-Biased MEMS Sensor Array

This sensor array was designed to perform spectral decomposition of acoustic emission signals generated specifically during impact events, as illustrated in Figure 2. The sensor array would be bonded to a high acoustic impedance material with a spherical surface profile on the impacting surface. An acoustic pulse is generated when this sensor module impacts a flat second material. The width of that pulse, representing its spectral content, depends on the acoustic impedance of the two materials involved. The sensor array was designed to distinguish between those different impact scenarios.

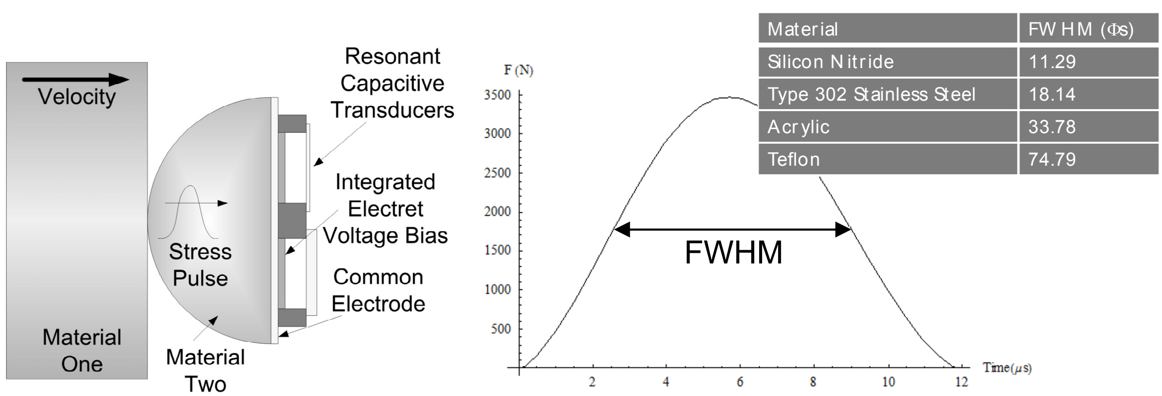

Figure 2: Sensor Array Operation in an Impact Environment

For demonstration purposes, natural frequencies for the individual transducers in the array were selected to cover a range from 10kHz to 100kHz. A single chip contained seven individual transducer elements, with each sensor suspended above its own charged electret area. The largest structure was 2mm by 2mm. Each subsequent structure was reduced in size by 200μm. The Nickel used in these structures was intended to be 10μm thick, had a density of 8900 kg/m^3 and had an elastic modulus of 221 GPa. Figure 3 shows the layout of a full sensor chip consisting of these multiple bridges, with lengths varying from 800μm to 2mm, suspended over interconnected charging grids.

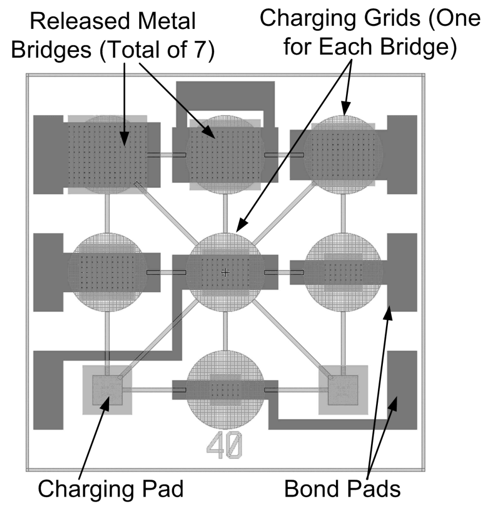

Length (mm)	*Resonant Frequency*
2.0	12.812 kHz
1.8	15.817 kHz
1.6	20.018 kHz
1.4	26.146 kHz
1.2	35.558 kHz
1.0	51.247 kHz
0.8	80.074 kHz

Figure 3: An entire array of sensors is fabricated with interconnected embedded microcorona charging grids. Each sensor in the array has a metal bridge with a natural frequency ranging from 10kHz to 100kHz.

3. SENSOR FABRICATION

Sensor fabrication is based on an *in situ* electret formation using microcorona discharge. Microcorona discharges have been previously achieved in microfabricated structures [9, 10, 11]. We demonstrate the use of this phenomenon for *in situ* charging of electrets and electret arrays. CYTOP [12], a thermoplastic fluoropolymer encapsulant for electronics, is used as the polymer electret film because it can be spin-cast, has a high resistivity, and is easily etched in oxygen plasma. Figure 4 shows a fabrication process and cross-section for an *in situ* charging grid comprising multiple micro corona electrodes. The grid structure is conceptually similar to the corona wires in copy machines and laser printers. The grid consists of multiple thin-film metal edges suspended a short distance above the polymer film. When energized by a high voltage, the sharp metal edges lead to high dielectric fields that ionize the air in the gap and force electric charge onto the polymer surface. In this work, the grid consisted of an array of narrow lines, approximately 5μm wide, and separated by an approximately 40μm gap. The metal of the grid is first deposited directly on the polymer, patterned, and then "suspended" approximately 2μm above the polymer film by isotropically etching the polymer out from underneath it.

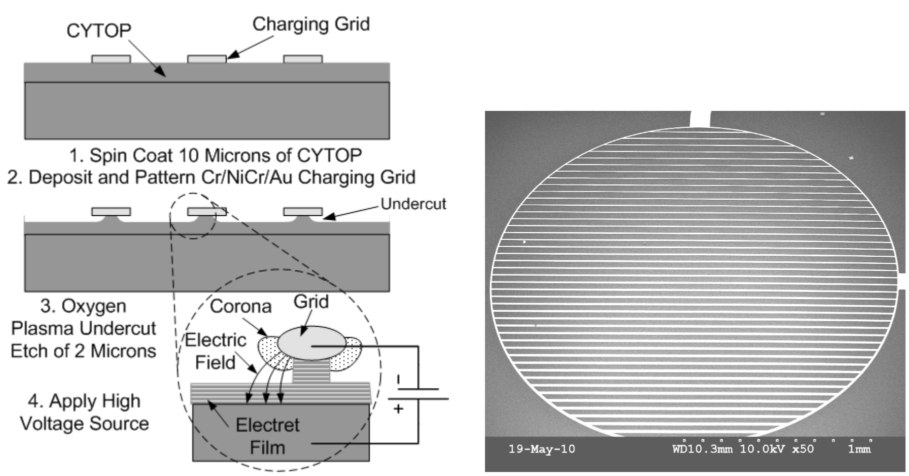

Figure 4: Miniature MicroCorona Charging Grids

After fabrication of the charging grid, additional microfabrication steps, as shown in Figure 5, are performed to build the acoustic sensor array [13]. SU8 is first spin-coated over the charging grids and a pattern of posts is exposed. The SU8 is not immediately developed, but instead undergoes a 12 hour post-exposure bake. After the bake, the wafer is coated with

Cr using a low-power e-beam evaporator. The low-power deposition minimizes SU8 crosslinking during the deposition. Following Cr deposition, a layer of gold is deposited. A photoresist plating mold is then spin-coated and patterned, followed nickel electroplating. Finally, the photoresist mold and the undeveloped SU8 are removed using a series of acetone and developer baths, yielding a fully released structure. An SEM image of a final sensor device with a charging grid is shown in Figure 6.

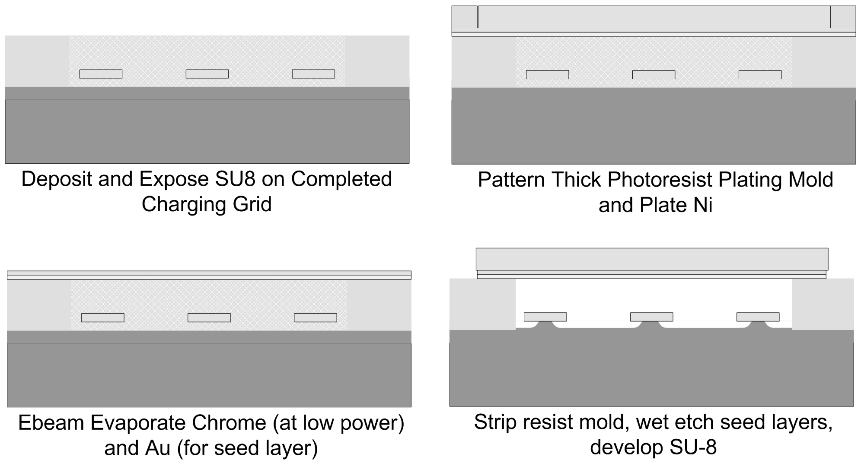

Figure 5: The full sensor fabrication process builds the micromechanical sensor element above the unpolarized polymer electret film. All of the fabrication steps, including structure release, are performed prior to in situ polarization of the film.

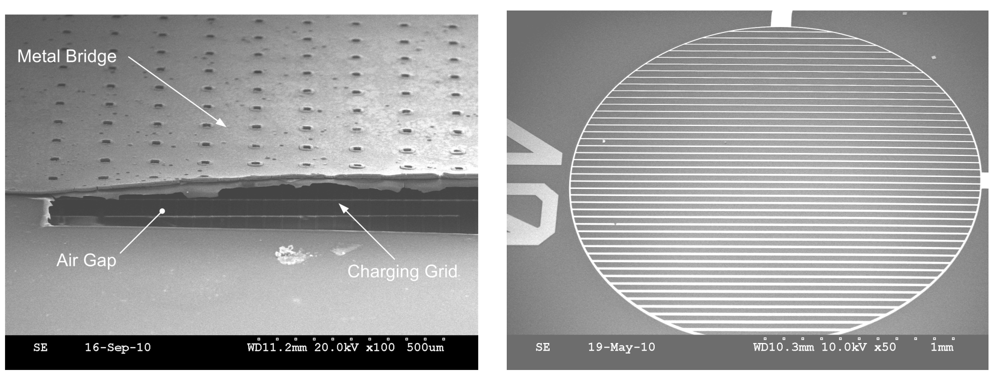

Figure 6: (a) An SEM image shows a close-up view of a fabricated charging grid underneath the suspended metal bridge. Imperfections in the release process for the SU8 material led to film residue on the structure.(b) An SEM image of a completed charging grid

In a finished device, after the MEMS structure is released, the electret formation process is performed by energizing the grid to a high negative voltage. When a suitable potential is achieved across the air gap between the grid and the polymer film surface, a microcorona discharge occurs. Ions travel to the polymer surface where they transfer their charge. The charge builds up until sufficient potential is achieved such that the microcorona no longer exists. Actual charged sites achieved an electrostatic voltage of approximately -200V after the first charging cycle.

4. SENSOR CHARACTERIZATION

In the sensor array, a metal bridge transducer is suspended above each charging site; with each individual transducer in the array designed to exhibit a different natural frequency. This array was designed to perform spectral decomposition of an incident acoustic wave, with the natural frequencies spanning the range from 10kHz to 100kHz. When an impact or vibration is experienced, the output of the array represents a measurement of the spectrum of that input source. For this purpose, the natural frequency of the sensor element, as well as its sensitivity to the acoustic displacement, must be characterized. Therefore, after fabrication and polarization, a sensor die was driven by a piezoelectric sheet in the test configuration shown in Figure 7. The sensor die was coupled to the piezoelectric sheet using coupling oil, while the piezoelectric sheet was coupled to a Teflon block. The piezoelectric sheet was driven by an external function generator while the output from each individual sensor element was amplified and captured with an oscilloscope. The drive frequency of the piezoelectric sheet was scanned from 10kHz to 100kHz while the amplitude of the sensor output was recorded. Figure 7 shows a representative scan of the sensor response for the lowest frequency device in the array. Each sensor element exhibited a higher natural frequency than as designed. This is likely due to the characteristics of the Nickel film, including the curvature induced by the Nickel stress. After characterization, some additional mass was added to the lowest frequency device to lower its natural frequency. Figure 7 also lists the final natural frequencies of each element in the array as determined through this characterization process.

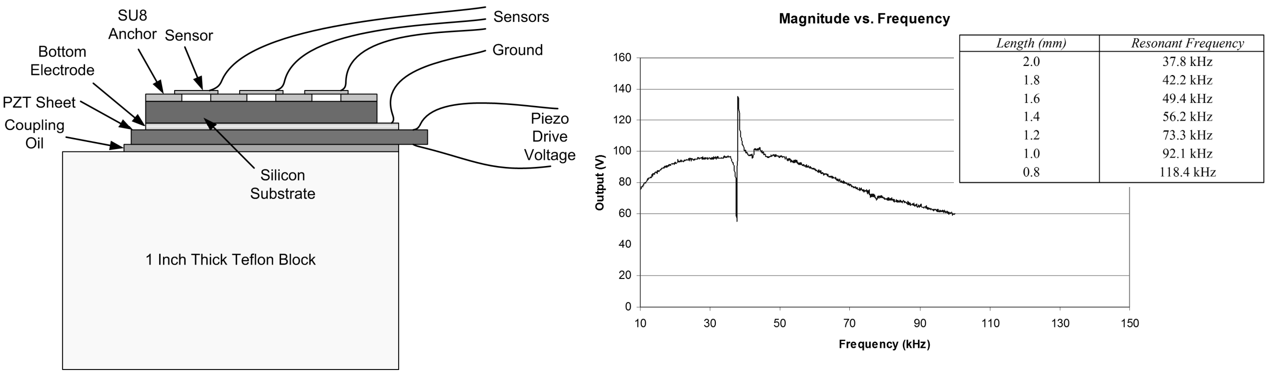

Length (mm)	Resonant Frequency
2.0	37.8 kHz
1.8	42.2 kHz
1.6	49.4 kHz
1.4	56.2 kHz
1.2	73.3 kHz
1.0	92.1 kHz
0.8	118.4 kHz

Figure 7: Sensor Array Calibration after Fabrication, Release, and Electret Formation

After individual element characterization, the sensor array was incorporated into a drop tower impact system. Figure 8 shows the sensor array attached to a hemispherical Alumina structure and impacted by a projectile. Four projectiles with identical geometries, but made up of different materials, were dropped on to the hemisphere from a constant height. The materials used in the test were selected to provide a range of acoustic impedances, and included Teflon, acrylic, stainless steel, and silicon nitride. Figure 8 also shows maximum peak voltage for each sensor from impacts between cylindrical projectiles of different materials and a ceramic hemi-sphere on which the sensor array is mounted. Hertzian contact theory [14] indicates that each material would present a unique signature across the frequency spectrum.

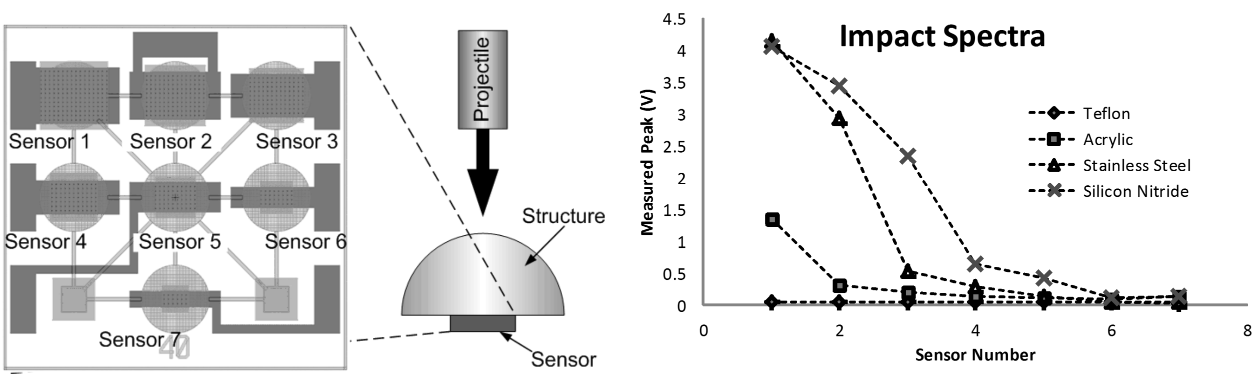

Figure 8: Sensor Array and Impact Test Setup

This sensor array demonstrates the utility of *in situ* electret formation within the structures, and that multiple sites could be charged with the application of voltage to a single contact pad, allowing the approach to be scaled to a full wafer implementation. This sensor array also demonstrated the ability to distinguish, through the use of multiple tuned sensor elements, between the acoustic signals generated during the impact of the structure with different materials.

5. CONCLUSIONS

In situ charging of electret areas within a MEMS acoustic emission sensor array using microplasma discharges, and the operation of that sensor array as a mechanical signal process tool was presented in this paper. The electret integration approach that enables array formation is based on the fabrication of micro charging grids embedded within the MEMS structure during MEMS fabrication. After completing the fabrication flow and releasing the structure, energizing the embedded grid leads to electrostatic discharge from the metal edges of the grid to the electret film surface, leading to charge transfer and film polarization similar to the traditional macro-scale corona discharge process. In contrast, the *in situ* process can be performed after entire MEMS structure fabrication and release, thereby mitigating high-temperature process issues that electret films often experience. The process can also be scaled to the wafer-level, with multiple independent electret sites formed simultaneously within device.

The in situ polarization process was incorporated into a MEMS ultrasonic sensor array device to demonstrate embedded mechanical spectral decomposition of acoustic emission signals. These sensor arrays demonstrate sensitivity to ultrasonic waves, as well as the separate of frequency components in the ultrasonic signals through the use of a range of natural frequencies within the array. When incorporated into an impact scenario, the array devices were able to distinguish between impacts of different materials without the need for analog sampling, digital conversion, and digital signal processing. The resulting sensor array operated on small amounts of power and fit within a small footprint. Potential signal processing issues seen in the array included the need to calibrate individual elements after fabrication, shifts in sensor calibration over temperature and time, coupling of electrical signals between elements of the array, and varying levels of sensitivity across the array. These issues will be explored in future work.

REFERENCES

[1] Whitley, M, Kranz, M., "Latching Shock Sensors for Health Monitoring and Quality Control," *SPIE Photonics West*, (2005).

[2] E. Cretu, L.A. Rocha, and R.F. WolffenButtel, "Electro-Mechanical Feedback for Realization of a Mechanical Spectrum Analyzer," *Transducers '03*, 3E60.P, (2003).

[3] Suzuki, H., Kinjo, T., Hayashi, Y., Takemoto, M., and Ono, K., "Wavelet Transform of Acoustic Emission Signals." *Journal of Acoustic Emission*, 14, No. 2, 69-84, (1996).

[4] Ozevin, D., Greve, D. W. , Oppenheim, I. J. , and Pessiki, S. P. , "Resonant capacitive MEMS acoustic emission transducer," *Smart Materials Struct*ures, **15**, 1863-1871, (2006).

[5] Goel, M., "Electret sensors, filters and MEMS devices: New challenges in materials research," Current Science, Vol. 85, No. 4, 25 August, (2003).

[6] Hsu, T.-H., Yeh, C.-N., and Su, Y.-C., "Piezoelectric PDMS Electrets for MEMS Transducers," *IEEE MEMS 2010*, Hong Kong, January 25-28, (2010).

[7] Sterken, T., Baert, K., Puers, R., Borghs, S., "Power extraction from ambient vibration," *Proceedings of the Workshop on Semiconductor Sensors*, November 29, (2002), Veldhoven, the Netherlands, p. 680-683.

[8] Halvorsen, E., Westby, E. R., Husa, S., Vogl, A., Østbø, N.P., Leonov, V., Sterken, T., and Kvisterøy, T., "An Electrostatic Energy Harvester with Electret Bias", *Transducers 2009*, Denver, CO, June 21-25, (2009).

[9] Lee, S., Kim, D., Bryant, M. D., Ling, F., "A Micro Corona Motor," Sensors and Actuators A, 118, (2005), pp. 226-232.

[10] Wilson, C. G., and Gianchandani, Y. B., "Silicon Micromachining Using *In Situ* DC Microplasmas," Journal of Microelectromechanical Systems, Vol. 10, No. 1, March, (2001).

[11] Honzumi, M., Ueno, A., Hagiwara, K., Suzuki, Y., "Soft-X-Ray-Charged Vertical Electrets and Its Application to Electrostatic Transducers," *23rd IEEE International Conference on MEMS (MEMS 2010)*, Hong Kong, January , (2010).

[12] Sakane, Y., Suzuki, Y., and Kasagi, N., "The development of a high-performance perfluorinated polymer electret and its application to micro power generation," Journal of Micromechanics and Microengineering, 18 (2008) 104011 (6pp) 29 September 2008

[13] Chung, C., and Allen, M., "Uncrosslinked SU-8 as a Sacrificial Material," *Journal of Micromechanics and Microengineering*, 15, pp. N1-N5, (2005).

[14] Gachagan, A., Mulholland, A. J., Hayward, G., Tramontana, M., Nordon, A., Carson, G. "Particle Sizing in the Process Industry using Hertz-Zener Impact Theory and Acoustic Emission Spectra," *Ultrasonics Symposium*, 2006, Page(s):1406 – 1409, October (2006).